ISSN 1063-7826, Semiconductors, 2013, Vol. 47, No. 7, pp. 987–992. © Pleiades Publishing, Ltd., 2013.
Original Russian Text © O.Ya. Olikh, 2013, published in Fizika i Tekhnika Poluprovodnikov, 2013, Vol. 47, No. 7, pp. 979–984.

PHYSICS OF SEMICONDUCTOR DEVICES

Effect of Ultrasonic Loading on Current in Mo/n–n^+-Si with Schottky Barriers

O. Ya. Olikh

Taras Shevchenko National University of Kyiv, Kyiv, 01601 Ukraine

e-mail: olikh.univ.kiev.ua

Submitted October 4, 2012; accepted for publication October 20, 2012

Abstract—The results obtained in experimental studies of the operation of silicon Schottky diodes subjected to ultrasonic loading (oscillations frequency of 9.6 MHz; intensity of longitudinal waves as high as 0.7 W/cm^2) are reported. A reversible acoustically induced decrease in the Schottky barrier height (to 0.13 V) and an increase in the saturation and reverse current (by as much as 60%) are observed. It is shown that ultrasound does not affect the ideality factor of the diodes and the tunneling component of the reverse current. The process of electron transport is considered within the context of the model of an inhomogeneous Schottky barrier; it is shown that the observed effects can be related to the acoustically induced ionization of defects, which are located at the metal–semiconductor interface.

DOI: 10.1134/S106378261307018X

1. INTRODUCTION

Recently, much attention has been given to studies of the possibility of using acoustic waves as an active instrument for affecting the defect system and, consequently, the operating characteristics of semiconductor devices. The following specific features can be included in the advantages of the suggested method compared to annealing or irradiation:

(i) Absorption of ultrasound occurs predominantly in regions, where there is a deviation in the periodicity of the crystal; as a result, the effect is more localized.

(ii) The use of waves with different polarization and types makes it possible to increase the selectivity of the effect.

(iii) By selecting the oscillation frequency, one can attain resonance transformations in the defect subsystem.

The possibility of the effective use of ultrasound for affecting the properties of various semiconductors and devices based on them is confirmed by available experimental data (for example, [1–16]). Among other things, the ultrasound effect can give rise to a variation in the parameters of barrier semiconductor devices, for example, this effect can give rise to improvement in the photoelectric parameters of solar cells [6, 7], result in a decrease in the charge-carrier concentration [8], an increase in the tunneling component of the current [9] in p–n junctions, and a variation in the current–voltage (I–V) characteristics of structures with a Schottky barrier [10–13].

It is worth noting that the predominant number of publications is concerned with residual effects observed as a result of the long-term (10^3–10^4 s) and high-power (as a rule, the ultrasound intensity is no lower than 1 W/cm^2) acoustic effect. At the same time, in our opinion, the most promising in terms of practical implementation is the use of ultrasound for a dynamic (reversible) variation in semiconductor devices during their operation. In particular, under such conditions, the crystals are often found in a nonequilibrium state and their defect–impurity subsystem can be modified under the effect of ultrasound with a much lower intensity. In addition, in this situation, we can find a way for the fabrication of some devices of functional acoustoelectronics, in which the parameters of the information signal are controlled by the dynamic inhomogeneities of the medium; these inhomogeneities arise due to the effect of a controlling acoustic signal. The possibility of implementing such an approach is confirmed by the results published in [7, 14–16], where acoustodynamic effects in semiconductors and the effects of ultrasound on nonequilibrium charge carriers are described. Publications concerned with acoustoelectric phenomena in Schottky diodes (SDs) are practically lacking.

The aim of this study was experimental investigation of dynamic variations in silicon SDs under conditions of ultrasonic loading and investigation of the causes of acoustic effects.

2. EXPERIMENTAL

The studied structures consisted of an n^+-Si:Sb substrate with a resistivity of 0.01 Ω cm and a thickness of 250 μm and also an n-Si:P epitaxial layer

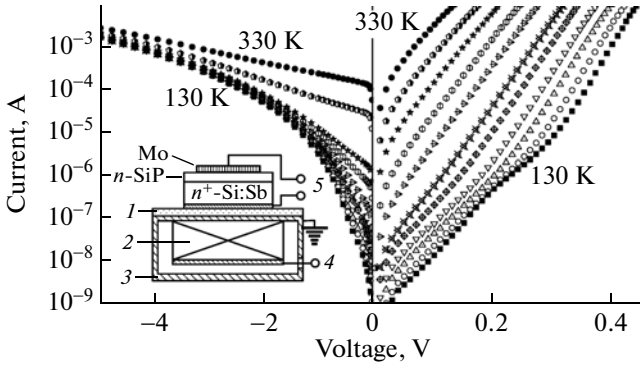

Fig. 1. Current–voltage characteristics of Mo/n–n^+-Si Schottky diodes in the temperature range 130–330 K. Curves measured with a step of 20 K are shown. The inset shows the schematic representation of ultrasonic loading of the sample: *1* is the insulator layer; *2* is the $LiNbO_3$ piezoelectric converter; *3* is the screening layer; and *4* and *5* are the electrodes for the excitation of ultrasound and measurement of the current–voltage characteristic, respectively. The total thickness of the insulating and screening layers is 0.02 mm.

(carrier concentration $N_D = 1.3 \times 10^{23}$ m^{-3} and a thickness of ~0.2 μm), on the surface of which a Schottky contact with a diameter of 2 mm was formed by depositing a molybdenum layer; an ohmic contact was formed on the opposite side of the substrate. The doping profile of the sample was determined by measuring the capacitance–voltage (C–V) characteristics at room temperature. Such structures are used in the commercial fabrication of rectifying diodes, in particular, of the 2D219 type.

In the study under consideration, the I–V characteristics were measured in the range of 120–330 K and also under conditions of ultrasonic loading at room temperature. In the case of ultrasonic loading, longitudinal waves with a frequency f_{us} equal to 9.6 and 30.1 MHz and with an intensity of $W_{us} < 0.7$ W/cm^2 were excited in the samples. A schematic representation of the ultrasonic loading is shown in the inset in Fig. 1; the method itself is described in more detail in [17].

Examples of the forward and reverse I–V characteristics are shown in Fig. 1. It is known [18, 19] that the dependence of the current I through the Schottky contact on the applied forward voltage can be described by the relation

$$I = I_s \exp\left(\frac{q(V - IR_s)}{nk_BT}\right)\left[1 - \exp\left(-\frac{q(V - IR)}{k_BT}\right)\right], \quad (1)$$

where I_s is the saturation current, n is the ideality factor, q is the elementary charge, k_B is the Boltzmann constant, T is temperature, and R_s is the series resistance. In this study, for determination of I_s and n the dependence of the experimental quantity

$$\ln\left(I/\left\{1 - \exp\left[-\frac{q(V - IR_s)}{k_BT}\right]\right\}\right)$$

on V was constructed; then, this dependence was approximated with a straight line whose angular coefficient and free term made it possible to determine the values of the desired quantities. It is worth noting that the value $R_s \le 0.5\ \Omega$ obtained using Gromov's method [19] indicates that this resistance is related to the ohmic contacts. It can be seen from Fig. 1 that an excess current is observed in the forward I–V characteristics at low temperatures ($T < 230$ K) and small biases (corresponding to $I < 5 \times 10^{-6}$ A). In order to exclude the effect of this current in determining the values of I_s and n, the portions of the I–V characteristics with $I > 10^{-5}$ A were used in the approximation. It is noteworthy that the ultrasonic loading was performed at room temperature.

In determining the Schottky barrier height (SBH) at zero bias Φ_b, the following expression [18] was used:

$$\Phi_b = \left(\frac{k_BT}{q}\right)\ln\left(\frac{AA^*T^2}{I_s}\right). \quad (2)$$

Here, A is the contact area (3.14×10^{-6} m^2) and A^* is the effective Richardson constant ($A^* = 112$ A cm^{-2} K^{-2} for n-Si [20]).

In order to exclude the effect of a piezoelectric field on the I–V characteristic during the course of ultrasonic loading, the piezoelectric cell was shielded (see the inset in Fig. 1). In addition, to separate the effects of sign-alternating strain and heating, which accompanies ultrasonic loading, on the SD parameters (I_s, n, Φ_b, and the reverse current), a special procedure of measuring and result processing was used. This procedure was described in detail in [7] and included determination of the temperature dependences of the diode characteristics, control of sample temperature during ultrasonic loading, and calculation of variations in the parameters with corrections due to heating taken into account.

3. EXPERIMENTAL RESULTS AND DISCUSSION

3.1. Forward Current–Voltage Characteristics

The aim of measuring the I–V characteristics in a wide temperature range consisted in the identification of the charge-transport mechanisms; it is impossible to analyze the causes of the ultrasound effect on the structural parameters without understanding the above mechanisms. For example, studies have shown that, for the samples under consideration, the value of Φ_b increases as the temperature is increased (see Fig. 2).

Such behavior is contradictory both in terms of what is expected within the context of Bardeen's model, which takes into account the effect of surface states at the interface on the barrier height [18], and experimental results [21, 22] obtained for structures with a homogeneous Schottky barrier (SB). Thus, in order to explain the obtained results, it is necessary to use another approach, for example, the model of an inhomogeneous SB [23, 24]; recently, the latter model has been often [25–29] utilized in analyzing the I–V characteristics of real metal–semiconductor structures. For example, according to [23], in the case of the Gaussian distribution of the SBH over the contact area, the following relations should be valid for Φ_b and n in the context of thermionic-emission theory:

$$\Phi_b = \Phi_b^0 - \frac{q\sigma_\Phi^2}{2k_BT}, \quad (3)$$

$$(n^{-1} - 1) = \rho_2 - \frac{q\rho_3}{2k_BT}. \quad (4)$$

Here, Φ_b^0 is the average value of the SBH, σ_Φ is the standard deviation of the SBH (this parameter characterizes the homogeneity of the contact), and ρ_2 and ρ_3 are the parameters describing the variation in the SBH under the effect of bias. As can be seen from Fig. 2, the linear dependence of Φ_b and n on the inverse temperature is observed for the samples under study in two different temperature ranges: 120–220 K and 230–330 K. It is worth noting that such variation in the slope of the dependences of Φ_b and n on $(k_BT)^{-1}$ was observed previously [25—27]. The values of the parameters obtained by linear approximation of the dependences in Fig. 2 according to (3) and (4) are listed in the table.

In the context of another model considered in [24], it is assumed that the SBH remains constant over the entire contact, except for small local regions (LRs), where the barrier height is smaller; it is the presence of these LRs that gives rise to inhomogeneity in the SB in general. In this case, the dependence of Φ_b on n must be linear [24, 28], which is exactly observed in the case under consideration (see the inset in Fig. 2). It is noteworthy that different linear portions are observed in the same temperature ranges as those in the dependences of Φ_b and n on $(k_BT)^{-1}$.

Various LRs can differ from each other in terms of size and barrier height. It was shown in [29] that (i), in this case, the relation (3) should also be valid with Φ_b^0 having the meaning of the SBH beyond a LR, while σ_Φ is related to a spread in the LR parameters; and (ii) the temperature dependence of the nonideality factor can be described by the expression

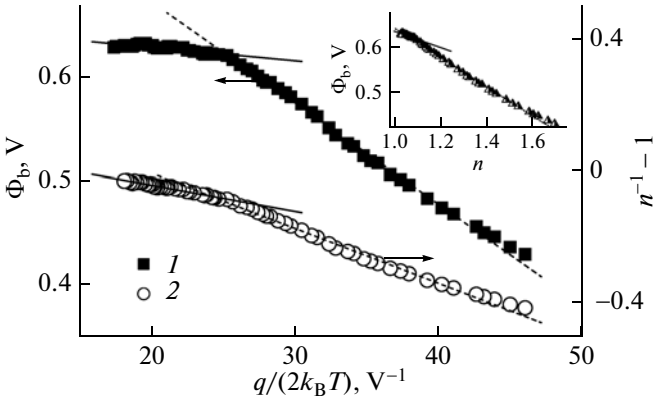

Fig. 2. Dependences of the value of Φ_b (curve *1*) and $(n^{-1} - 1)$ (*2*) on the inverse temperature. The inset shows the dependence of the Schottky barrier height on the nonideality factor n. The symbols are experimental. The straight lines are linear approximations in the range of 230–330 K (continuous curve) and 120–220 K (dashed curves).

$$n = 1 + (T_0/T) \quad (5)$$

with

$$T_0 = \frac{q\sigma_\Phi^2}{3k_BV_{bb}}, \quad (6)$$

where $V_{bb} = \Phi_b^0 - V_n - V$, while $V_n = (k_BT/q)\ln(N_c/N_D)$, where N_c is the effective density of states near the conduction-band bottom.

The obtained experimental dependence $n(T)$ at $T <$ 260 K is also satisfactorily described by expression (5) with $T_{0,\,exp} = 12$ K. On the other hand, direct calculation based on expression (6) with the values of Φ_b^0- and σ_Φ obtained for the range (230–330) K yields the value $T_{0,\,theor} \approx 11$ K, which is close to $T_{0,\,exp}$; this represents still more evidence of the correctness of using the model of the inhomogeneous contact for the structures under study.

In the case of an inhomogeneous SB, the Richardson constant can be estimated by plotting the temper-

Parameters of Mo/n-Si structures determined via the model of a homogeneous Schottky barrier

Range of temperatures	Φ_b^0, mV	σ_Φ, mV	ρ_2, 10^{-2}	ρ_3, mV	A^*_{exp}, 10^6 A cm^{-2} K^2
120–220	872 ± 4	99 ± 1	33 ± 1	17.0 ± 0.3	122 ± 20
230–330	663 ± 3	40 ± 5	12 ± 1	8.0 ± 0.3	112 ± 20

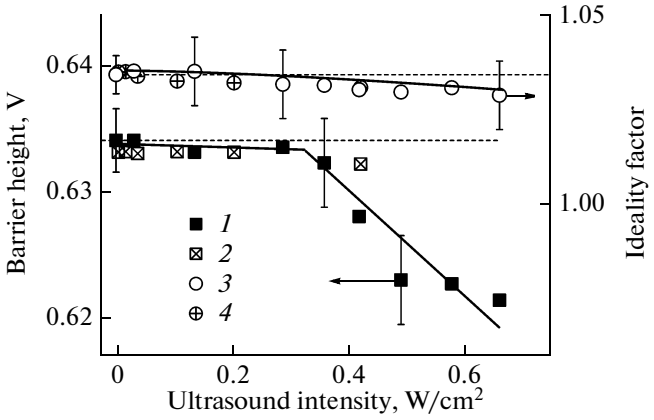

Fig. 3. Dependences of the Schottky barrier height (curves *1*, *2*) and the ideality factor (*3*, *4*) on the intensity of ultrasonic loading at $T = 296$ K, $f_{us} = 9.6$ (*1*, *3*) and 30.1 (*2*, *4*) MHz. Horizontal dashed lines represent the values of the parameters in the absence of ultrasonic loading.

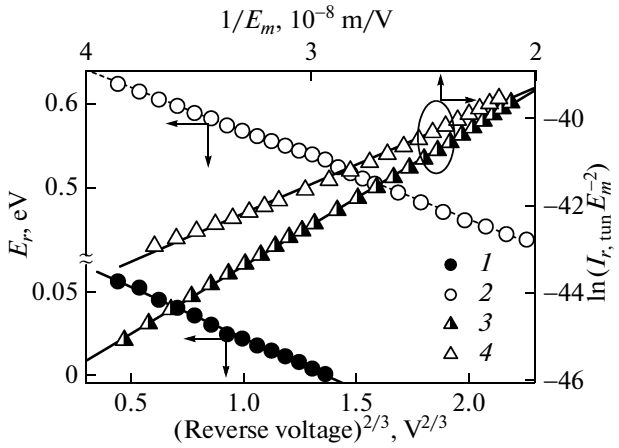

Fig. 4. Field dependences of the characteristic energy (curves *1*, *2*) and the temperature-independent component of the reverse current in Fowler–Nordheim coordinates (*3*, *4*) at $T = 120$–220 K (*1*, *3*) and $T = 230$—330 K (*2*, *4*). The symbols represent the experimental data, and the straight lines, the linear approximations.

ature dependence of $\ln(I_s/T^2) - q^2\sigma_\Phi^2/(2k_B^2T^2)$ since, according to [25, 26],

$$\ln(I_s/T^2) - q^2\sigma_\Phi^2/(2k_B^2T^2) = \ln(AA^*) - q\Phi_b^0/(k_BT). \quad (7)$$

The values of A^*_{exp} obtained by linear approximation of the dependence (7) are listed in the table. It is worth noting that the experimental quantities A^*_{exp} are close to those listed in the literature.

Finally, the appearance of excess currents, similar to those observed in the case under consideration (Fig. 1) is expected to take place in the model of the LR inhomogeneous barrier [24] at low temperatures and low biases.

Thus, all obtained results indicate that, in the samples under consideration, the forward current can be described within the context of thermionic emission through an inhomogeneous SB.

Figure 3 shows the dependences, which illustrate the behavior of Φ_b and n under conditions of ultrasonic loading. It should be emphasized that, as was already stated above, the ultrasound intensity was comparatively low and, as a result, all acoustically induced variations in the parameters of the structures under study (Figs. 3, 5) featured a reversible character, i.e., they relaxed after the cessation of ultrasonic loading in a time on the order of ten minutes.

As can be seen from Fig. 3, a decrease in the SBH is observed under conditions of ultrasonic loading; at $W_{us} \approx 0.66$ W/cm^2, $\Delta\Phi_b = \Phi_{b,\,us} - \Phi_{b,\,0} \approx -(13 \pm 4)$ mV (here, $\Phi_{b,\,0}$ and $\Phi_{b,\,us}$ are the values of the SBH before/after and during ultrasonic loading). It is worth noting that the use of the subscripts "0" and "us" for various quantities implies that the conditions are the same for them. Some threshold is observed in the amplitude dependence; this threshold corresponds to the value $W_{us} \approx 0.35$ W/cm^2. It is noteworthy that a frequency dependence of the ultrasound-effect efficiency in Schottky diodes was not observed, in contrast to previously studied silicon solar cells [7].

It follows from formula (3) that the cause of a variation in the barrier height can be the effect of ultrasound on Φ_b^0 or σ_Φ. As follows from formulas (3), (5), and (6), in the case where, under conditions of ultra-

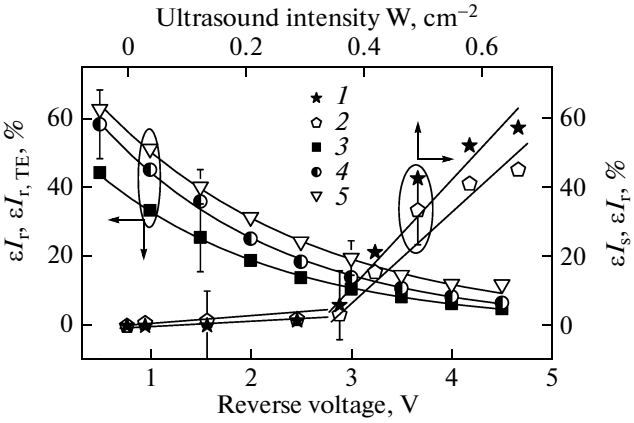

Fig. 5. Dependences of relative acoustically induced variations in the saturation current (curve *1*) and the reverse current at $V_r = 1$ V (*2*) on the intensity of ultrasonic loading and also the dependences of relative acoustically induced variations in the reverse current (*3*, *4*) and the relative contribution of the thermionic effect to the total reverse current (*5*) on the reverse bias W_{us} = (*3*) 0.49, (*4*) 0.66, and (*5*) 0 W/cm^2. $f_{us} = 9.6$ MHz. $T = 296$ K.

sonic loading, the value of Φ_b^0 remains unchanged, the variation in the nonideality factor must be described by the relation

$$\Delta n(\Phi_b^0 = \text{const}) = n_{us} - n_0 = -\frac{2\Delta\Phi_b}{3V_{bb}}.$$

If, in contrast, the value of σ_Φ remains unchanged, then

$$\Delta n(\sigma_\Phi = \text{const}) = -\frac{q\sigma_\Phi^2\Delta\Phi_b}{3k_BTV_{bb,us}V_{bb,0}}.$$

The calculations performed using the values of $\Delta\Phi_b = -0.013$ V and $V = 0.1$ V and the data of the table show that $\Delta n(\Phi_b^0 = \text{const}) \approx 0.02$ and $\Delta n(\sigma_\Phi = \text{const}) \approx 0.002$. Thus, if ultrasonic loading affects the LR parameters (the value of σ_Φ), an appreciable increase in the nonidealty factor is bound to be observed. At the same time, the almost total lack of acoustically induced variations in n is experimentally observed (Fig. 3; curves *3*, *4*); this is indicative of, first, the lack of the effect of ultrasonic loading on LRs and, second, a decrease in the value of the SBH in the homogeneous part of the contact in an acoustic field.

As is known [18, 30], in the context of Bardeen's theory, the SBH can be described by the expression

$$\Phi_b^0 = \gamma(\Phi_m - \chi) + (1-\gamma)\left[\frac{E_g}{q} - \varphi_0\right], \quad (8)$$

where $\gamma = 1/[1 + q\delta D_s/(\varepsilon\varepsilon_0)]$, Φ_m is the work function of the metal, χ is the electron affinity, E_g is the band gap, φ_0 is the neutrality level measured from the valence-band top (the level below which all surface states should be occupied so that the surface is electrically neutral), δ is the thickness of the oxide interface layer, D_s is the density of states at the interface, ε_0 is the permittivity of free space, and ε is the dimensionless permittivity (for Si, $\varepsilon = 11.7$). Since the acoustically-induced effects are reversible, it is impossible to relate them to variations in the value of D_s. Consequently, the cause of a decrease in the SBH under ultrasonic loading is, most probably, an increase in φ_0 as a result of, for example, the acoustically-induced ionization of defects at the interface. It is most likely that such defects can be dislocations, which appear during epitaxy and SB formation. In the context of this assumption, the threshold behavior and the frequency independence of variations in the SBH can be accounted for: the efficiency of oscillations in dislocations in the ultrasonic field significantly increases as they are released from stoppers and for the used frequency range barely depend on the oscillation period. It is noteworthy that the acoustically-induced effects of defect ionization, including dislocations at the interface of the barrier structures, were observed previously [7, 31].

3.2. Reverse Current–Voltage Characteristics

It can be seen from Fig. 1 that the reverse I–V characteristics cannot be adequately described in the context of the model of thermionic emission through the barrier with the height constant at the given temperature. In order to determine the mechanisms of charge transport, the approximation of experimental dependences of the value of the reverse current I_r at different biases V_r was performed using the expression

$$I_r(T, V_r = \text{const}) = I_{r,TE} + I_{r,tun} = CT^2\exp\left[-\frac{E_r}{k_BT}\right] + I_{r,tun}, \quad (9)$$

where the first term $I_{r,TE} = CT^2\exp[-E_r/(k_BT)]$ describes the thermionic component of the current while the second term describes the temperature-independent current component; the parameters E_r (related to the barrier height) and C are also temperature independent. As in the case of the analysis of the forward portions of the I–V characteristics, the approximation was performed separately in the ranges of 120–220 and 230–330 K. As can be seen from Fig. 4, the characteristic energy E_r depends linearly on $V_r^{2/3}$. Such a dependence indicates that the component $I_{r,TE}$ is related to thermionic processes of transmission through the inhomogeneous SB since, according to [24], the barrier height is bound to decrease exactly in proportion to $V_r^{2/3}$ in the presence of LRs with different parameters.

Figure 4 also shows the field dependences of $I_{r,tun}$ plotted in Fowler–Nordheim coordinates $\ln(I_{r,tun}/E_m^2) = f(E_m^{-1})$, where $E_m = [2qN_DV_{bb}/(\varepsilon\varepsilon_0)]^{1/2}$ is the electric-field strength at the metal–semiconductor interface [18]; the above-obtained values of Φ_b^0 and the value of V_n at $T = 250$ K were used in the calculations of E_m. The linearity of the dependences is indicative of the tunneling mechanism of current $I_{r,tun}$ flow [32], which is also confirmed by the temperature independence of the value of $I_{r,tun}$.

Thus, the reverse current through the structures under study is determined by the processes of both tunneling and thermionic emission through the inhomogeneous SB. It is found that relative contribution of each component depends on the bias voltage; for example, Figure 5 (curve *5*) shows the dependence for the value of $\varepsilon I_{r,TE} = I_{r,TE}/(I_{r,TE} + I_{r,tun})$.

Under conditions of ultrasound loading, an increase in the value of the reverse current is observed. The character of the ultrasound effect on the reverse and forward currents is similar both qualitatively and quantitatively. For example, Fig. 5 shows the amplitude dependences of relative variations in the reverse

current $\varepsilon I_r = (I_{r,us} - I_{r,0})/I_{r,0}$ and in the saturation current $\varepsilon I_s = (I_{s,us} - I_{s,0})/I_{r,0}$ (curves *1*, *2*). In addition, the dependence of variations in the reverse current on the bias voltage (Fig. 5; curves *3*, *4*) is practically identical to the dependence of $\varepsilon I_{r,TE}$. Thus, a variation in the reverse current as a result of ultrasonic loading is related to the effect on thermionic processes and is accounted for by a decrease in the SBH, as was described above.

The fact that ultrasonic loading does not affect the tunneling component of current is indicative of the selectivity of the ultrasound effect, which is not characteristic of more traditional methods for modification of the parameters of semiconductor structures. For example, as a result of the irradiation of SB-containing structures based on *n*-Si with ions or electrons, the reverse current increases and Φ_b decreases; however, the appearance of radiation defects intensifies tunneling processes [33–35]. Consequently, ultrasonic loading can be considered as a tool for the directional effect on certain parameters of metal–semiconductor structures.

4. CONCLUSIONS

It is shown that the temperature dependences of the *I–V* characteristics in Mo/n–n^+-Si structures indicate that the Schottky barrier is inhomogeneous and also that the reverse current is determined by both thermionic and tunneling processes.

The effect of ultrasonic loading under dynamic conditions on the Schottky-diode parameters was experimentally studied for the first time. It was found that, in the course of the propagation of acoustic waves, a reversible decrease in the SBH and an increase in the reverse and saturation currents is observed; at the same time, the nonideality factor remains practically unchanged. It is shown that ultrasonic loading does not affect the parameters of local regions, which give rise to contact inhomogeneity; the observed effects can be accounted for by the acoustically induced ionization of defects located at the interface. It is found that ultrasonic loading barely affects the tunneling component of the reverse current.

The results of this study can be used in the development of acoustically controlled diodes of various types.

REFERENCES

1. A. El-Bahar, S. Stolyarova, A. Chack, R. Weil, R. Beserman, and Y. Nemirovsky, Phys. Status Solidi A **197**, 340 (2003).
2. E. M. Zobov, M. E. Zobov, F. S. Gabibov, I. K. Kamilov, F. I. Manyakhin, and E. K. Naimi, Semiconductors **42**, 277 (2008).
3. P. B. Parchinskii, S. I. Vlasov, and L. G. Ligai, Semiconductors **40**, 808 (2006).
4. A. Romanyuk, P. Oelhafen, R. Kurps, and V. Melnik, Appl. Phys. Lett. **90**, 013118 (2007).
5. M. Jivanescu, A. Romanyuk, and A. Stesmans, J. Appl. Phys. **107**, 114307 (2010).
6. E. B. Zaveryukhina, N. N. Zaveryukhina, L. N. Lezilova, B. N. Zaveryukhin, V. V. Volodarskii, and R. A. Muminov, Tech. Phys. Lett. **31**, 27 (2005).
7. O. Ya. Olikh, Semiconductors **45**, 798 (2011).
8. A. Davletova and S. Zh. Karazhanov, J. Phys. D: Appl. Phys. **41**, 165107 (2008).
9. A. V. Sukach and V. V. Teterkin, Tech. Phys. Lett. **35**, 514 (2009).
10. O. Ya. Olikh and T. N. Pinchuk, Tech. Phys. Lett. **32**, 517 (2006).
11. M. B. Tagaev, Ukr. Fiz. Zh **45**, 364 (2000).
12. I. G. Pashaev, Semiconductors **46**, 1085 (2012).
13. A. M. Gorb, O. A. Korotchenkov, O. Ya. Olikh, and A. O. Podolian, IEEE Trans. Nucl. Sci. **57**, 1632 (2010).
14. Ya. M. Olikh and N. D. Timochko, Tech. Phys. Lett. **37**, 37 (2011).
15. O. Ya. Olikh, Semiconductors **43**, 745 (2009).
16. B. N. Zaveryukhin, N. N. Zaveryukhina, R. A. Muminov, and O. M. Tursunkulov, Tech. Phys. Lett. **28**, 207 (2002).
17. O. Ya. Olikh, Ukr. Fiz. Zh. **55**, 770 (2010).
18. E. H. Roderick and R. H. Williams, *Metal-Semiconductor Contacts* (Clarendon, Oxford, 1988; Radio i svyaz', Moscow, 1982).
19. D. Gromov and V. Pugachevich, Appl. Phys. A **59**, 331 (1994).
20. D. K. Schroder, *Semiconductor Material and Device Characterization* (Wiley, New Jersey, 2006), p. 158.
21. S. Zhu, R. L. van Meirhaeghe, C. Detavernier, G.-P. Ru, B.-Z. Li, and F. Cardon, Solid State Commun. **112**, 611 (1999).
22. M. O. Aboelfotoh, J. Appl. Phys. **66**, 262 (1989).
23. J. H. Werner and H. H. Guttler, J. Appl. Phys. **69**, 1522 (1991).
24. R. T. Tung, Phys. Rev. B **45**, 13509 (1992).
25. I. Tascioglu, U. Aydemir, and S. Altındal, J. Appl. Phys. **108**, 064506 (2010).
26. N. Yıldırım, K. Ejderha, and A. Turut, J. Appl. Phys. **108**, 114506 (2010).
27. M. Mamor, J. Phys.: Condens. Matter **21**, 335802 (2009).
28. K. Sarpatwari, S. E. Mohney, and O. O. Awadelkarim, J. Appl. Phys. **109**, 014510 (2011).
29. F. Iucolano, F. Roccaforte, F. Giannazzo, and V. Raineri, J. Appl. Phys. **102**, 113701 (2007).
30. H. Ikoma, T. Ishida, K. Sato, and T. Ishikawa, J. Appl. Phys. **73**, 1272 (1993).
31. O. A. Korotchenkov and H. G. Grimmliss, Phys. Rev. B. **52**, 14598 (1995).
32. A. Evtukh, E. Kaganovich, E. Manailov, and N. Semenenko, Semiconductors **40**, 175 (2006).
33. S. Kumar, Y. S. Katharria, and D. Kanjilal, J. Phys. D: Appl. Phys. **41**, 105105 (2008).
34. A. Rao, S. Krishnan, G. Sanjeev, and K. Siddappa, Int. J. Pure Appl. Phys. **5**, 55 (2009).
35. R. Singh, S. K. Arora, and D. Kanjilal, Mater. Sci. Semicond. Process. **4**, 425 (2001).

Translated by A. Spitsyn